

Tuning the Magnetic Quantum Criticality of Artificial Kondo Superlattices CeRhIn₅/YbRhIn₅

T. Ishii,¹ R. Toda,¹ Y. Hanaoka,¹ Y. Tokiwa,^{1,2} M. Shimozawa,³ Y. Kasahara,¹ R. Endo,¹ T. Terashima,^{2,*}
A. H. Nevidomskyy,⁴ T. Shibauchi,⁵ and Y. Matsuda¹

¹Department of Physics, Kyoto University, Kyoto 606-8502, Japan

²Research Center for Low Temperature and Materials Science, Kyoto University, Kyoto 606-8501, Japan

³Institute for Solid State Physics, University of Tokyo, Kashiwa 277-8581, Japan

⁴Department of Physics and Astronomy, Rice University, 6100 Main Street, Houston, Texas 77005, USA

⁵Department of Advanced Materials Science, University of Tokyo, Chiba 277-8561, Japan

(Received 10 March 2016; published 20 May 2016)

The effects of reduced dimensions and the interfaces on antiferromagnetic quantum criticality are studied in epitaxial Kondo superlattices, with alternating n layers of heavy-fermion antiferromagnet CeRhIn₅ and seven layers of normal metal YbRhIn₅. As n is reduced, the Kondo coherence temperature is suppressed due to the reduction of effective Kondo screening. The Néel temperature is gradually suppressed as n decreases and the quasiparticle mass is strongly enhanced, implying dimensional control toward a quantum critical point. Magnetotransport measurements reveal that a quantum critical point is reached for the $n = 3$ superlattice by applying small magnetic fields. Remarkably, the anisotropy of the quantum critical field is opposite to the expectations from the magnetic susceptibility in bulk CeRhIn₅, suggesting that the Rashba spin-orbit interaction arising from the inversion symmetry breaking at the interface plays a key role for tuning the quantum criticality in the two-dimensional Kondo lattice.

DOI: [10.1103/PhysRevLett.116.206401](https://doi.org/10.1103/PhysRevLett.116.206401)

In Kondo lattices consisting of a periodic array of localized spins that are coupled to conduction electrons, a very narrow conduction band is formed at sufficiently low temperatures through the Kondo effect [1]. Such systems are realized in intermetallic heavy-fermion metals, which contain a dense lattice of certain lanthanide ($4f$) and actinide ($5f$) ions. In particular, in Ce($4f$)-based compounds, strong electron correlations strikingly enhance the quasiparticle (QP) effective mass to about 100 or more times the bare electron mass, resulting in a heavy Fermi liquid state. In the strongly correlated electron systems, non-Fermi liquid behavior, associated with the quantum fluctuations near a quantum critical point (QCP), a point at which a material undergoes a second-order transition from one phase to another at absolute zero temperature [2], has been one of the central issues. The heavy-fermion systems are particularly suitable for this study, because the ground state can be tuned readily by control parameters other than temperature, such as magnetic field, pressure, or chemical substitution [3]. As a result of the many-body effects within the narrow band in these heavy-fermion compounds, a plethora of fascinating properties have been reported in the vicinity of a QCP.

Recently, a state-of-the-art molecular beam epitaxy (MBE) technique has been developed to fabricate an artificial Kondo superlattice, a superlattice with alternating layers of Ce-based heavy-fermion compounds and nonmagnetic conventional metals that are a few atomic layers thick [4]. These artificially engineered materials provide a new platform to

study the properties of two-dimensional (2D) Kondo lattices, in contrast to the three-dimensional bulk materials. In the previously studied CeCoIn₅/YbCoIn₅ superlattices [4], where CeCoIn₅ is a heavy-fermion superconductor and YbCoIn₅ is a conventional metal, each Ce block layer (BL) is magnetically decoupled from the others, since the Ruderman-Kittel-Kasuya-Yoshida interaction between the spatially separated Ce BLs is negligibly small due to the presence of the nonmagnetic spacer Yb BLs. Moreover, the large Fermi velocity mismatch across the interface between heavy-fermion and nonmagnetic metal layers significantly reduces the transmission probability of heavy QPs [5]. In fact, it has been shown that the superconducting heavy QPs as well as the magnetic fluctuations are well confined within the 2D Ce BLs, as revealed by recent studies of the upper critical field and site-selective nuclear magnetic resonance [6,7]. Quantum fluctuations are expected to be more pronounced in reduced spatial dimensions [8], and the artificial Kondo superlattices therefore have an advantage to extend the quantum critical regime without long-range ordering. On the other hand, although the previous studies on CeCoIn₅/YbCoIn₅ superlattices pointed out the importance of the interface between the heavy-fermion and the adjacent normal-metal BLs [9–11], the question of how the interface affects quantum critical phenomena still remains largely unexplored.

Here, to study the magnetic quantum criticality of 2D Kondo lattices, we have fabricated superlattices of CeRhIn₅(n)/YbRhIn₅(7), formed by alternating layers

of heavy-fermion CeRhIn₅ [12–14] and normal metal YbRhIn₅ [15]. Bulk CeRhIn₅ shows a long-range antiferromagnetic (AFM) order below $T_N = 3.8$ K at ambient pressure; it orders in an incommensurate magnetic structure with ordering vector $\mathbf{q} = (1/2, 1/2, 0.297)$ [16]. The magnetic order is suppressed by applying pressures and the ground state becomes purely superconducting at $p > p^* \approx 1.95$ GPa with most likely d -wave symmetry, similarly to CeCoIn₅ [17] and CeIrIn₅ [18]. Compared to the previously studied CeIn₃/LaIn₃ superlattices [4] based on the cubic heavy-fermion antiferromagnet CeIn₃ with a higher $T_N = 10$ K and $\mathbf{q} = (1/2, 1/2, 1/2)$ [19], the effect of reduced dimensionality would be more prominent in the present superlattices based on the tetragonal CeRhIn₅ with a lower T_N . We show that the reduced dimensionality, achieved by reducing n , leads to the appearance of the QCP at $n \approx 3$. Remarkably, quantum fluctuations in the $n = 3$ superlattice are sensitive to the applied magnetic field and its direction. Based on these results, we discuss the significant effect of the inversion symmetry breaking at the interface on the magnetic quantum criticality in the 2D Kondo lattice.

The CeRhIn₅(n)/YbRhIn₅(7) Kondo superlattices used for this work were epitaxially grown on a MgF₂ substrate using the MBE technique [4]. We first grew CeIn₃ (~ 20 nm) as a buffer layer, on top of which seven layers of YbRhIn₅ and n layers of CeRhIn₅ were stacked alternatively, in such a way that the total thickness was about 300 nm (see the inset in Fig. 1). Figure 1 shows the temperature dependence of the resistivity $\rho(T)$ of the $n = 9, 5, 4,$ and 3 superlattices, along with the CeRhIn₅ thin film (300 nm). The resistivity of the thin film reproduces well that of a single crystal. In the thin film and $n = 9$ superlattice, the Kondo coherence temperature T_{coh} is estimated from the maximum in $\rho(T)$ after subtracting the resistivity of nonmagnetic LaRhIn₅ [20] to account for the phonon contribution. The $\rho(T)$ data in the $n = 5, 4,$ and 3 superlattices show a maximum at T_{coh} without any background subtraction. As shown in the inset of Fig. 1, T_{coh} decreases with increasing $1/n$, indicating that reduced dimensionality dramatically suppresses the Kondo coherence [21]. It is unlikely that the crystal electric field at the Ce site changes significantly in the superlattices, because it is mainly determined by the neighboring Ce, In, and Rh ions. Therefore, the observed suppression of T_{coh} in the superlattices is a many-body effect likely due to the reduction of the effective number of the conduction electrons that participate in the Kondo screening.

It has been reported that the temperature derivative of the resistivity, $d\rho/dT$, exhibits a sharp peak at T_N in bulk CeRhIn₅. Figure 2(a) depicts $d\rho/dT$ at low temperatures for the thin film and the superlattices. In the thin film, $d\rho/dT$ reproduces that of the bulk, indicating the AFM transition at $T_N = 3.8$ K [14]. A distinct peak is also observed in the $n = 9, 5,$ and 4 superlattices, suggesting

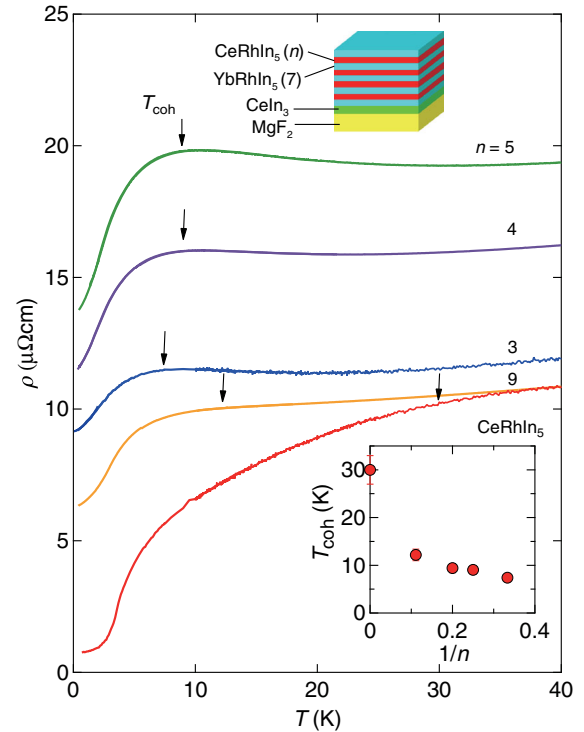


FIG. 1. Temperature dependence of resistivity ρ for the CeRhIn₅ thin film and CeRhIn₅(n)/YbRhIn₅(7) superlattices. The arrows indicate the Kondo coherence temperature T_{coh} . Top inset: a schematic representation of the superlattice. Bottom inset: T_{coh} as a function of $1/n$.

the presence of AFM order. For the $n = 3$ superlattice, on the other hand, the peak is very broad, and, thus, the determination of T_N is ambiguous, which will be discussed later. Obviously, the approach to two dimensions yielded by reducing n enhances quantum fluctuations and thus reduces T_N . To see whether the resistivity obeys the Fermi-liquid expression $\rho = \rho_0 + AT^2$, where ρ_0 is the residual resistivity and A is the Fermi liquid coefficient, the resistivity at low temperatures is plotted as a function of T^2 in Fig. 2(b). The resistivity of the thin film and $n = 9, 5,$ and 4 superlattices are well fitted by $\rho \propto T^2$ in a wide temperature range. On the other hand, as shown in the inset of Fig. 2(b), the T^2 dependence is observed only at very low temperatures for the $n = 3$ superlattice, consistent with approaching a QCP.

Figure 3 depicts the thickness dependence of T_N and A that is related to the QP effective mass m^* through the effective specific heat coefficient $\gamma_{\text{eff}} \propto m^*$ and the Kadowaki-Woods Fermi liquid relation $A/\gamma_{\text{eff}}^2 = 1 \times 10^{-5} \mu\Omega\text{cm}(\text{mol K/mJ})^2$ [22]. Concomitantly with the disappearance of T_N near $n = 3$, A is strikingly enhanced, by about 20 times its magnitude in the bulk. It is natural to consider that the mass enhancement and the deviation from the Fermi liquid behavior of the resistivity for the $n = 3$ superlattice are caused by the quantum critical fluctuations

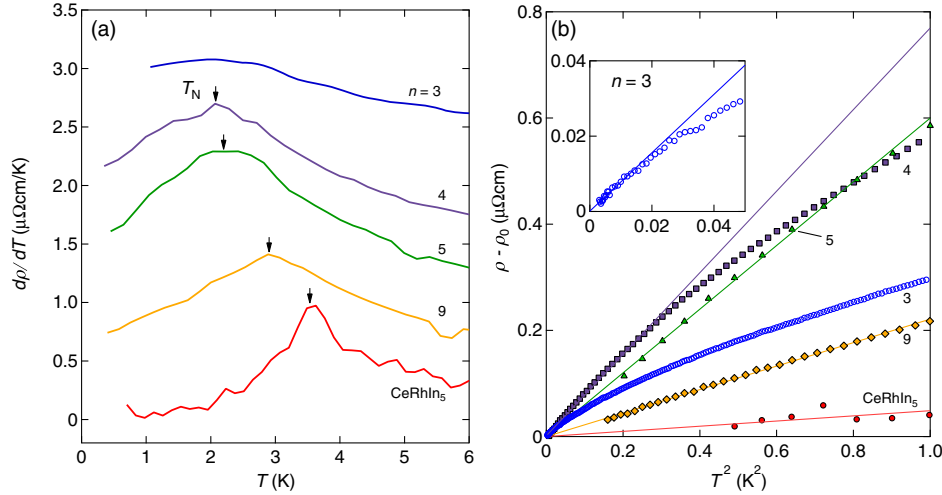


FIG. 2. (a) Temperature derivative of the resistivity, $d\rho/dT$, as a function of T for the CeRhIn_5 thin film and $\text{CeRhIn}_5(n)/\text{YbRhIn}_5(7)$ superlattices. The arrows indicate the Néel temperature T_N . (b) $\rho - \rho_0$ plotted against T^2 . The solid lines are the fits to the T^2 dependence at the lowest temperatures. The inset displays $\rho - \rho_0$ vs T^2 for the $n = 3$ superlattice at low temperatures.

associated with the QCP in the vicinity of $n = 3$, i.e., dimensional tuning of the quantum criticality.

To further elucidate the nature of the QCP, we study the magnetoresistance and its anisotropy in an applied magnetic field. Figures 4(a) and 4(b) show the evolution of α , the exponent in $\rho(T) - \rho_0 = \Delta\rho(T) \propto T^\alpha$, within the field-temperature (B - T) phase diagram of the $n = 3$ superlattice, for the magnetic field applied parallel to the ab plane and c axis, respectively. For both field directions, the exponent α at low temperatures is strongly affected by the magnetic field [23–25]. At $B_c \approx 1.2$ T for $\mathbf{B} \parallel ab$ and $B_c \approx 2$ T for $\mathbf{B} \parallel c$, the non-Fermi liquid behavior ($\alpha \lesssim 1.5$) is observed down to the lowest temperatures and in a largely extended field range at higher temperatures. For $B > B_c$, a broad

crossover regime from the non-Fermi liquid state to the field-induced Fermi liquid state at lower temperature is found to occur. Thus, the non-Fermi liquid behavior dominates over a funnel shaped region of the B - T phase diagram for both field directions. We note that similar phase diagrams have been reported in the bulk heavy fermion compound YbRh_2Si_2 [23], which constitutes one of the best studied examples of quantum criticality. In Figs. 4(a) and 4(b), the field dependence of γ_{eff} for the $n = 3$ superlattice estimated from the T^2 -dependent resistivity in the Fermi liquid regime is also plotted. As the field approaches B_c from either side, γ_{eff} is rapidly enhanced. These results corroborate the emergence of a field-induced

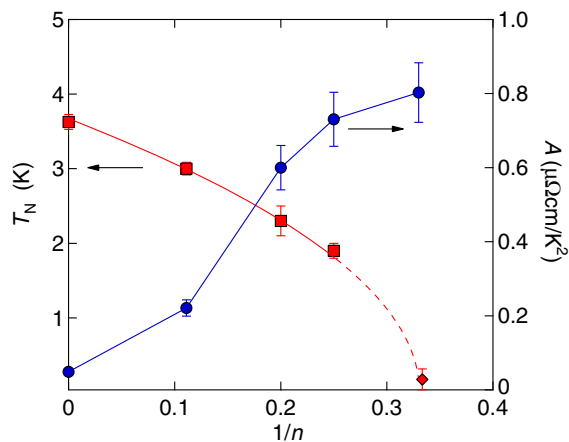


FIG. 3. The Néel temperature T_N (left axis) and Fermi liquid coefficient A derived from the expression $\rho = \rho_0 + AT^2$ as a function of $1/n$. T_N for the $n = 3$ superlattice (diamond) is estimated by the temperature below which the Fermi liquid behavior is observed.

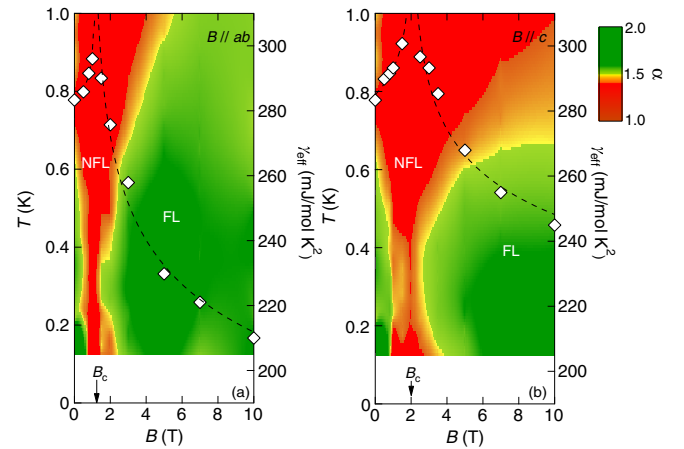


FIG. 4. Temperature and magnetic field evolution of the exponent α derived from the expression $\rho(T) = \rho_0 + AT^\alpha$ in the $n = 3$ superlattice (a) for $\mathbf{B} \parallel ab$ and (b) for $\mathbf{B} \parallel c$. The triangles represent the effective specific heat γ_{eff} estimated from the resistivity at the lowest temperatures assuming the T^2 -dependent resistivity (right axis).

QCP at B_c . Although $d\rho/dT$ does not show a discernible peak for the $n = 3$ superlattice in Fig. 2(a), the Néel temperature is roughly estimated to be $T_N \sim 0.16$ K by the temperature below which the Fermi liquid behavior is observed [see the inset of Fig. 2(b)]. We conclude that in the present 2D Kondo lattice, quantum fluctuations are sensitive to the applied magnetic field; fields of about 1 T are sufficient to induce a QCP, above which the Fermi liquid state with a strongly field-dependent QP mass appears. This small B_c is in sharp contrast to the magnetic field of ≈ 50 T required to suppress T_N in bulk CeRhIn₅ [26].

The quantum fluctuations are also sensitive to the field direction. It should be noted that in bulk CeRhIn₅, the magnetic susceptibility perpendicular to the ab plane is much larger than that parallel to the plane, $\chi_c \gg \chi_{ab}$ [13], implying that the field response for $\mathbf{B} \parallel ab$ is expected to be much less sensitive than that for $\mathbf{B} \parallel c$, similar to the case of YbRh₂Si₂ where the magnitudes of B_c for the different field directions are proportional to the magnetic anisotropy. What is remarkable is that, as seen from Figs. 4(a) and 4(b), the quantum fluctuations are more easily suppressed for $\mathbf{B} \parallel ab$ than for $\mathbf{B} \parallel c$. Thus, the anisotropy of the quantum critical field in the present 2D Kondo lattice is opposite to that of the bulk susceptibility. Interestingly, a recent high-field study of bulk CeRhIn₅ finds that the critical value of B_c at $T = 0$ is isotropic [26], although it has been reported that the suppression of T_N by a magnetic field occurs more rapidly for $\mathbf{B} \parallel c$ than for $\mathbf{B} \parallel ab$ at low fields, opposite to what we observe in Fig. 4.

To explain the observed anisotropy of the critical field, we point out the importance of the space inversion symmetry. Here, in the $n = 3$ superlattice, the inversion symmetry is locally broken at the top and bottom layers of the CeRhIn₅ blocks in the immediate proximity to the YbRhIn₅ layers, whereas the symmetry is preserved in the middle layer [7,9–11]. In the absence of inversion symmetry, the asymmetry of the potential in the direction perpendicular to the 2D plane $\nabla V \parallel [001]$ induces the Rashba spin-orbit interaction $\alpha_R \mathbf{g}(\mathbf{k}) \cdot \boldsymbol{\sigma} \propto (\mathbf{k} \times \nabla V) \cdot \boldsymbol{\sigma}$, where $\mathbf{g}(\mathbf{k}) = (k_y, -k_x, 0)/k_F$, k_F is the Fermi wave number, and $\boldsymbol{\sigma}$ is the vector of the Pauli matrices. The Rashba interaction splits the Fermi surface into two sheets with different spin structures. The energy splitting is given by α_R , and the spin direction is tilted into the plane, rotating clockwise in one sheet and anticlockwise in the other [27]. Since the noncentrosymmetric interface layers occupy two thirds of the CeRhIn₅ layers in the $n = 3$ superlattice, the local inversion symmetry breaking at the interfaces, which results in the Rashba spin-orbit splitting of the Fermi surface, has a significant impact on the magnetic properties. In fact, it has been reported that local inversion symmetry breaking strongly affects the superconducting and magnetic properties in CeCoIn₅/YbCoIn₅ superlattices, leading to the suppression of the Pauli paramagnetic pair breaking effect and magnetic fluctuations at the interface [7,9–11].

In the presence of the local inversion symmetry breaking at the interfaces, the magnetic anisotropy is expected to be modified. For $\mathbf{B} \perp ab$, the Zeeman splitting $h = g\mu_B J_z B$ enters the energy $\varepsilon_{\mathbf{k}}$ of QPs at the Fermi level quadratically alongside the Rashba interaction: $E_{\pm}(\mathbf{k}) = \varepsilon_{\mathbf{k}} \pm \sqrt{h^2 + \alpha_R^2 |\mathbf{g}(\mathbf{k})|^2}$. Therefore, for weak fields ($h \ll \alpha_R$, which is the case here), the Zeeman effect is quadratic rather than linear in field, and is therefore strongly suppressed. By contrast, for in-plane field $\mathbf{B} \parallel ab$, there is a component of \mathbf{B} parallel to the Rashba-induced spin $\mathbf{g}(\mathbf{k})$, and the Zeeman effect is stronger. Therefore, the magnetic susceptibility for $\mathbf{B} \perp ab$ is expected to be suppressed more strongly than for $\mathbf{B} \parallel ab$. We theoretically analyzed the anisotropy ratio of the magnetic susceptibility, χ_c/χ_{ab} , and found that $\chi_c/\chi_{ab} \sim (\chi_c/\chi_{ab})_{\text{bulk}} \times 12[\delta^2 + \mathcal{O}(\delta^3)]$, where $\delta = h/\alpha_R$. We note that the results are robust against the details of the many-body renormalization of the effective mass (see the Supplemental Material [28]). Realistic values of the Rashba interaction and material parameters of CeRhIn₅ lead to the estimate of δ in the range (0.02–0.1) for the field $B = 1$ T, yielding the anisotropy ratio $1/100 \lesssim \chi_c/\chi_{ab} \lesssim 1/10$ [28], which is opposite to the anisotropy of bulk CeRhIn₅. To confirm this reversed anisotropy of the magnetic susceptibility, more direct measurements that provide microscopic information of the magnetism at the interface, such as site selective nuclear magnetic resonance, are strongly desired.

In summary, to investigate the physical properties of the two-dimensional Kondo lattice, we fabricated CeRhIn₅(n)/YbRhIn₅(7) superlattices. As the CeRhIn₅ layer thickness is reduced, the effective Kondo screening is largely reduced and the system approaches a quantum critical point in the vicinity of $n = 3$. We find that the quantum critical fluctuations, responsible for the non-Fermi liquid behavior, are very sensitive to the applied magnetic field and its direction. Fields of about 1 T are sufficient to tune the system to the QCP, which is 2 orders of magnitude smaller than the bulk value. The opposite anisotropy of the quantum critical field between the bulk and the $n = 3$ superlattice suggests that the Rashba spin-orbit interaction, arising from the local inversion symmetry breaking at the interface, plays an essential role for the magnetism in this artificially engineered 2D Kondo lattice.

We thank Y. Yanase for valuable discussions. This work was supported by Grants-in-Aid for Scientific Research (KAKENHI) (No. 25220710, No. 15H02014, No. 15H02106, and No. 15H05457), and Grants-in-Aid for Scientific Research on Innovative Areas “Topological Materials Science” (No. 15H05852) and “3D Active-Site Science” (No. 26105004) from Japan Society for the Promotion of Science (JSPS). A. H. N. acknowledges the support of U.S. National Science Foundation Grant No. DMR-1350237 and is grateful for the hospitality of the Institute of Solid State Physics, University of Tokyo.

- *Present address: Department of Physics, Kyoto University, Kyoto 606-8502, Japan.
- [1] A. C. Hewson, *The Kondo Problem to Heavy Fermions* (Cambridge University Press, Cambridge, England, 1993).
- [2] S. Sachdev, *Quantum Phase Transition* (Cambridge University Press, Cambridge, England, 1999).
- [3] H. Löhneysen, A. Rosch, M. Vojta, and P. Wölfle, *Rev. Mod. Phys.* **79**, 1015 (2007).
- [4] H. Shishido, T. Shibauchi, K. Yasu, T. Kato, H. Kontani, T. Terashima, and Y. Matsuda, *Science* **327**, 980 (2010).
- [5] J.-H. She and A. V. Balatsky, *Phys. Rev. Lett.* **109**, 077002 (2012).
- [6] Y. Mizukami *et al.*, *Nat. Phys.* **7**, 849 (2011).
- [7] T. Yamanaka, M. Shimozawa, R. Endo, Y. Mizukami, H. Shishido, T. Terashima, T. Shibauchi, Y. Matsuda, and K. Ishida, *Phys. Rev. B* **92**, 241105(R) (2015).
- [8] P. Monthoux, D. Pines, and G. G. Lonzarich, *Nature (London)* **450**, 1177 (2007).
- [9] D. Maruyama, M. Sigrist, and Y. Yanase, *J. Phys. Soc. Jpn.* **81**, 034702 (2012).
- [10] S. K. Goh, Y. Mizukami, H. Shishido, D. Watanabe, S. Yasumoto, M. Shimozawa, M. Yamashita, T. Terashima, Y. Yanase, T. Shibauchi, A. I. Buzdin, and Y. Matsuda, *Phys. Rev. Lett.* **109**, 157006 (2012).
- [11] M. Shimozawa, S. K. Goh, R. Endo, R. Kobayashi, T. Watashige, Y. Mizukami, H. Ikeda, H. Shishido, Y. Yanase, T. Terashima, T. Shibauchi, and Y. Matsuda, *Phys. Rev. Lett.* **112**, 156404 (2014).
- [12] H. Hegger, C. Petrovic, E. G. Moshopoulou, M. F. Hundley, J. L. Sarrao, Z. Fisk, and J. D. Thompson, *Phys. Rev. Lett.* **84**, 4986 (2000).
- [13] T. Takeuchi, T. Inoue, K. Sugiyama, D. Aoki, Y. Tokiwa, Y. Haga, K. Kindo, and Y. Ōnuki, *J. Phys. Soc. Jpn.* **70**, 877 (2001).
- [14] G. Knebel, D. Aoki, J.-P. Brison, and J. Flouquet, *J. Phys. Soc. Jpn.* **77**, 114704 (2008).
- [15] Z. Bukowski, K. Gofryk, and D. Kaczorowski, *Solid State Commun.* **134**, 475 (2005).
- [16] W. Bao, P. G. Pagliuso, J. L. Sarrao, J. D. Thompson, Z. Fisk, J. W. Lynn, and R. W. Erwin, *Phys. Rev. B* **62**, R14621(R) (2000).
- [17] K. Izawa, H. Yamaguchi, Y. Matsuda, H. Shishido, R. Settai, and Y. Onuki, *Phys. Rev. Lett.* **87**, 057002 (2001).
- [18] Y. Kasahara, T. Iwasawa, Y. Shimizu, H. Shishido, T. Shibauchi, I. Vekhter, and Y. Matsuda, *Phys. Rev. Lett.* **100**, 207003 (2008).
- [19] J. M. Lawrence and S. M. Shapiro, *Phys. Rev. B* **22**, 4379 (1980).
- [20] H. Shishido *et al.*, *J. Phys. Soc. Jpn.* **71**, 162 (2002).
- [21] D. Groten, G. J. C. van Baarle, J. Aarts, G. J. Nieuwenhuys, and J. A. Mydosh, *Phys. Rev. B* **64**, 144425 (2001).
- [22] H. Kontani, *Rep. Prog. Phys.* **71**, 026501 (2008).
- [23] J. Custers, P. Gegenwart, H. Wilhelm, K. Neumaier, Y. Tokiwa, O. Trovarelli, C. Geibel, F. Steglich, C. Pépin, and P. Coleman, *Nature (London)* **424**, 524 (2003).
- [24] P. Gegenwart, J. Custers, C. Geibel, K. Neumaier, T. Tayama, K. Tenya, O. Trovarelli, and F. Steglich, *Phys. Rev. Lett.* **89**, 056402 (2002).
- [25] S. Kasahara, T. Shibauchi, K. Hashimoto, K. Ikada, S. Tonegawa, R. Okazaki, H. Shishido, H. Ikeda, H. Takeya, K. Hirata, T. Terashima, and Y. Matsuda, *Phys. Rev. B* **81**, 184519 (2010).
- [26] L. Jiao *et al.*, *Proc. Natl. Acad. Sci. U.S.A.* **112**, 673 (2015).
- [27] Y. A. Bychkov and E. I. Rashba, *JETP Lett.* **39**, 78 (1984).
- [28] See Supplemental Material at <http://link.aps.org/supplemental/10.1103/PhysRevLett.116.206401>, which includes Refs. [13,20,27,29–33], for the theoretical analysis of the anisotropic magnetic susceptibility in the CeRhIn₅(*n*)/YbRhIn₅(7) superlattices in the presence of the Rashba interaction due to local symmetry breaking.
- [29] J. Luo, H. Muneke, F. F. Fang, and P. J. Stiles, *Phys. Rev. B* **41**, 7685 (1990).
- [30] J. Nitta, T. Akazaki, H. Takayanagi, and T. Enoki, *Phys. Rev. Lett.* **78**, 1335 (1997).
- [31] T. Hassenkam, S. Pedersen, K. Baklanov, A. Kristensen, C. B. Sorensen, P. E. Lindelof, F. G. Pikus, and G. E. Pikus, *Phys. Rev. B* **55**, 9298 (1997).
- [32] G. Dresselhaus, *Phys. Rev.* **100**, 580 (1955).
- [33] K. Yamada and K. Yosida, *Prog. Theor. Phys.* **76**, 621 (1986).